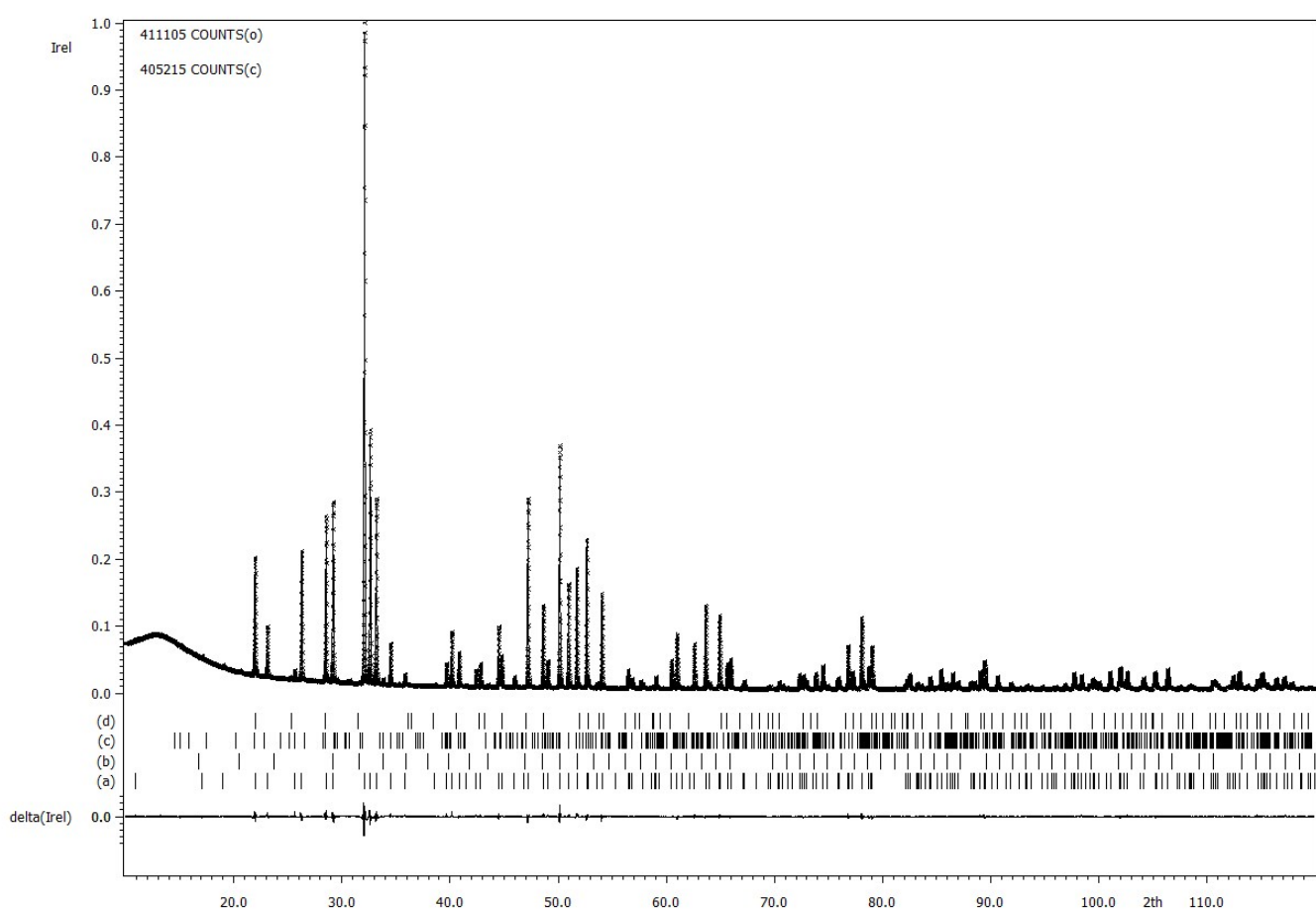


## Electronic supplementary information



**Figure S1.** X-ray powder diffraction pattern of  $\text{Y}_{7.75}\text{Dy}_{0.25}\text{Ca}_2(\text{SiO}_4)_6\text{O}_2$  (**1**). Observed (crosses), calculated (solid line) and difference (solid line below) plots. Positions of Bragg reflections are shown as strokes underneath. (a) the main apatite phase, (b)  $\text{Y}_2\text{O}_3$  (1.2 wt. %),  $\text{Y}_2\text{SiO}_5$  (1.4 wt. %), cristobalite  $\text{SiO}_2$  (2.4 wt. %).

**Table S1.** Crystal structure refinement data for **1**.

Temperature (K)	293 K
Wavelength (Å)	1.5406
Formula (refined)	$\text{Y}_{7.51}\text{Dy}_{0.24}\text{Ca}_{2.25}(\text{SiO}_4)_6\text{O}_2[\text{H}_6]$
Number of reflections	283
Number of data points	16749
Space group	P6 <sub>3</sub> /m
<i>a</i> (Å)	9.3474(2)
<i>c</i> (Å)	6.7830(1)
<i>V</i> (Å <sup>3</sup> )	513.25(2)
<i>Z</i>	1
2θ range (deg.)	10 – 120
<i>R</i> <sub>wp</sub>	0.032
<i>R</i> <sub>all</sub>	0.014
$\Delta F_{\max}$ , $\Delta F_{\min}$ (e Å <sup>-3</sup> )	0.31, -0.42

**Table S2.** Atomic parameters and thermal displacement parameters ( $\text{\AA}^2$ ) in **1**.

Atom	Y1 <sup>[a]</sup> , Ca1	Y2 <sup>[a]</sup> , Ca2	Si	O1	O2	O3	O4
Site	4f	6h	6h	6h	6h	12i	4e
SOF	0.564(8), 0.436(8)	0.916(10), 0.084(10)	1	1	1	1	1
<i>x</i>	1/3	0.00315(20)	0.3995(3)	0.3183(8)	0.6002(8)	0.3392(5)	0
<i>y</i>	2/3	0.23722(13)	0.3721(3)	0.4896(8)	0.4751(8)	0.2491(5)	0
<i>z</i>	0.0021(4)	1/4	1/4	1/4	1/4	0.0597(5)	0.25
<i>U</i> <sub>iso</sub>	0.0117(9)	0.0088(8)	0.0096(12)	0.010(2)	0.007(2)	0.0106(17)	0.014(3)

<sup>[a]</sup> Y1, Y2 was refined as a mixture Y<sub>0.96875</sub>Dy<sub>0.03125</sub>.

**Table S3.** Selected interatomic distances ( $\text{\AA}$ ) and angles (degrees) in the crystal structure of **1**.

Y1,Ca1-O1	2.314(6)	3x	Si-O1	1.621(10)
Y1,Ca1-O2	2.420(6)	3x	Si-O2	1.627(7)
Y1,Ca1-O3	2.784(5)	3x	Si-O3	1.631(4)
Y2,Ca2-O1	2.692(5)		O1-Si-O2	113.6(4)
Y2,Ca2-O2	2.368(11)		O1-Si-O3	111.4(3)
Y2,Ca2-O3	2.282(4)	2x	O2-Si-O3	107.7(3)
Y2,Ca2-O3	2.423(4)	2x	O3-Si-O3	104.7(3)
Y2,Ca2-O4	2.2026(15)			

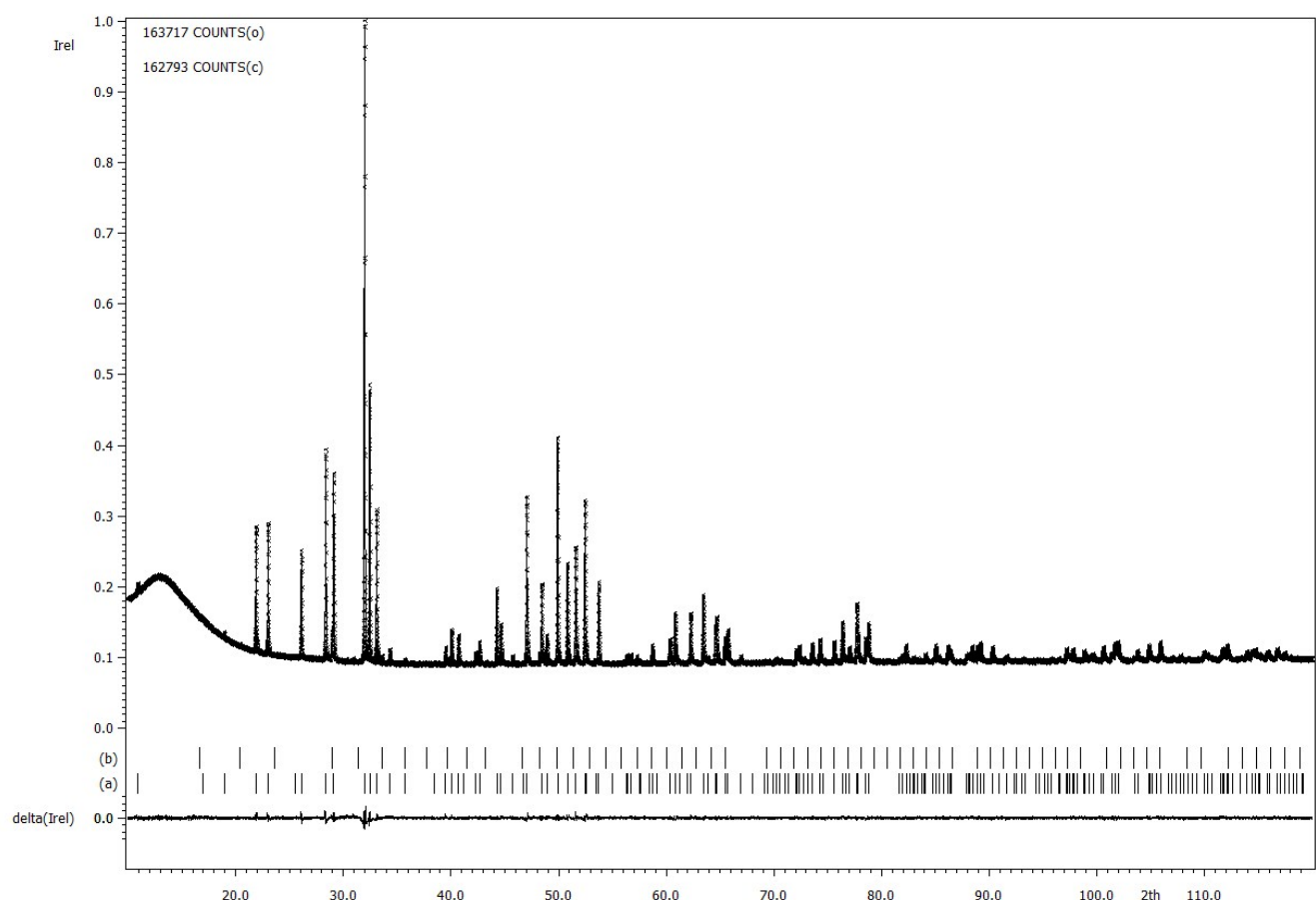


**Figure S2.** X-ray powder diffraction pattern of  $\text{Dy}_8\text{Ca}_2(\text{SiO}_4)_6\text{O}_2$  (**2**). Observed (crosses), calculated (solid line) and difference (solid line below) plots. Positions of Bragg reflections are shown as strokes underneath. (a) the main apatite phase, (b)  $\text{Dy}_2\text{O}_3$  (1.1 wt. %).

**Table S4.** Crystal structure refinement data for **2**.

Temperature (K)	293 K
Wavelength (Å)	1.5406
Formula (refined)	$\text{Dy}_{8.04}\text{Ca}_{1.96}(\text{SiO}_4)_6\text{O}_2$
Number of reflections	283
Number of data points	16749
Space group	$\text{P}6_3/\text{m}$
$a$ (Å)	9.3654(2)
$c$ (Å)	6.8188(1)
$V$ (Å <sup>3</sup> )	517.95(2)
$Z$	1
$2\theta$ range (deg.)	10 – 120
$R_{\text{wp}}$	0.011
$R_{\text{all}}$	0.020
$\Delta F_{\text{max}}, \Delta F_{\text{min}}$ (e Å <sup>-3</sup> )	0.48, -0.63

**Table S5.** Atomic parameters and thermal displacement parameters ( $\text{\AA}^2$ ) in **2**.

Atom	Dy1, Ca1	Dy2, Ca2	Si	O1	O2	O3	O4
Site	4f	6h	6h	6h	6h	12i	4e
SOF	0.594(7), 0.406(7)	0.944(10), 0.056(10)	1	1	1	1	1
<i>x</i>	1/3	0.0054(3)	0.3994(6)	0.3176(11)	0.6018(11)	0.3377(7)	0
<i>y</i>	2/3	0.23865(16)	0.3716(6)	0.4889(11)	0.4747(10)	0.2487(7)	0
<i>z</i>	-0.0002(7)	1/4	1/4	1/4	1/4	0.0609(7)	0.25
<i>U</i> <sub>iso</sub>	0.0101(9)	0.0069(6)	0.0078(18)	0.009(4)	0.003(3)	0.006(3)	0.008(4)

**Table S6.** Selected interatomic distances ( $\text{\AA}$ ) and angles (degrees) in the crystal structure of **2**.

Dy1,Ca1-O1	2.336(9)	3x	Si-O1	1.623(15)	
Dy1,Ca1-O2	2.414(9)	3x	Si-O2	1.642(10)	
Dy1,Ca1-O3	2.802	3x	Si-O3	1.630(6)	2x
Dy2,Ca2-O1	2.682(8)		O1-Si-O2	113.5(6)	
Dy2,Ca2-O2	2.372(15)		O1-Si-O3	110.9(4)	2x
Dy2,Ca2-O3	2.289(5)	2x	O2-Si-O3	108.2(4)	2x
Dy2,Ca2-O3	2.440(6)	2x	O3-Si-O3	104.6(4)	
Dy2,Ca2-O4	2.2103(19)				

**Table S7.** Crystal field parameters (in Wybourne notation) derived in the program CONCORD for Dy<sup>3+</sup> using experimental atomic coordinates of the coordination polyhedrons of Dy1 and Dy2 sites (from Table S5). Partial charges on the silicate oxygen atoms and on the intrachannel oxygen atom are -0.5 and -1.0 respectively (adjusted to fit the  $\chi T(T)$  dependence for 2).

Parameter	Value (cm <sup>-1</sup> )		
	Dy1 ( $a \rightarrow x, c \rightarrow z$ )	Dy2 ( $a \rightarrow x, c \rightarrow z$ )	Dy2 ( $z$ axis along easy magnetization axis)
B <sub>20</sub>	701.38363	-426.97211	993.34326
B <sub>22</sub>		-450.63672	56.914996
B <sub>40</sub>	-157.63795	157.89317	294.91316
B <sub>42</sub>		10.477190	-48.373936
B <sub>43</sub>	-54.565652		
B <sub>44</sub>		-131.48428	8.6605777
B <sub>60</sub>	-19.835861	-17.388239	41.718889
B <sub>62</sub>		-22.479997	-8.5295564
B <sub>63</sub>	-9.0345006		
B <sub>64</sub>		5.9183550	6.4517547
B <sub>66</sub>	1.9031082	14.562523	5.9352741
B <sub>21</sub>			
B <sub>41</sub>			
B <sub>61</sub>			
B <sub>65</sub>			
B <sub>21'</sub>		-84.160426	
B <sub>22'</sub>		-457.67948	
B <sub>41'</sub>		126.32885	
B <sub>42'</sub>		161.23726	
B <sub>43'</sub>	72.107571		-47.108550
B <sub>44'</sub>		90.664794	
B <sub>61'</sub>			-0.83957308
B <sub>62'</sub>		-12.005122	
B <sub>63'</sub>	20.817456		3.5214506
B <sub>64'</sub>		-8.0281853	
B <sub>65'</sub>			-10.676067
B <sub>66'</sub>	7.5849117	-5.8940102	

**Table S8.** Modeling with the program PHI using crystal field parameters listed in Table S7. The KDs of the ground multiplet  $^6\text{H}_{15/2}$  are shown only.

Dy1

Energy (cm <sup>-1</sup> )	$M_J$ (%)	$g_z$	$g_x$	$g_y$	Probability $M_J \rightarrow -M_J$
0	15/2 (99.97)	19.9976	0	0	
64.0008	13/2 (99.85)	17.2988	0.0001	0.0001	0.4501E-08
135.343	11/2 (99.64)	14.5908	0.0001	0.0001	0.1192E-05
204.748	9/2 (99.35)	11.8897	0	0	0.1182E-04
266.071	7/2 (98.99)	9.2065	0.0890	0.0890	0.2549E-02
315.214	5/2 (98.23)	6.5484	0.1024	0.1024	0.5682E-01
349.429	3/2 (94.50)	4.0055	0	0	0.2511E+00
366.971	1/2 (96.25)	10.6436	1.3030	10.6436	0.1819E+02

Dy2

Energy (cm <sup>-1</sup> )	$M_J$ (%)	$g_z$	$g_x$	$g_y$	Probability $M_J \rightarrow -M_J$
0	15/2 (100)	19.9994	0	0	
167.926	13/2 (99.87)	17.2872	0	0	0.7178E-03
298.260	11/2 (99.78)	14.6456	0.0009	0.0010	0.2984E-06
392.941	9/2 (98.49)	12.0443	0.0035	0.0059	0.2841E+00
456.651	7/2 (94.07)	9.1918	0.9112	1.2725	0.1201E+00
493.969	5/2 (68.07)	7.3280	4.3505	6.9856	0.8801E+01
	1/2 (22.07)				
526.148	3/2 (56.56)	14.0515	0.9259	2.0046	0.1735E+02
	-1/2 (14.91)				
	-5/2 (24.58)				
564.749	1/2 (62.31)	18.9301	0.0319	0.0653	0.3064E+02
	-3/2 (30.75)				

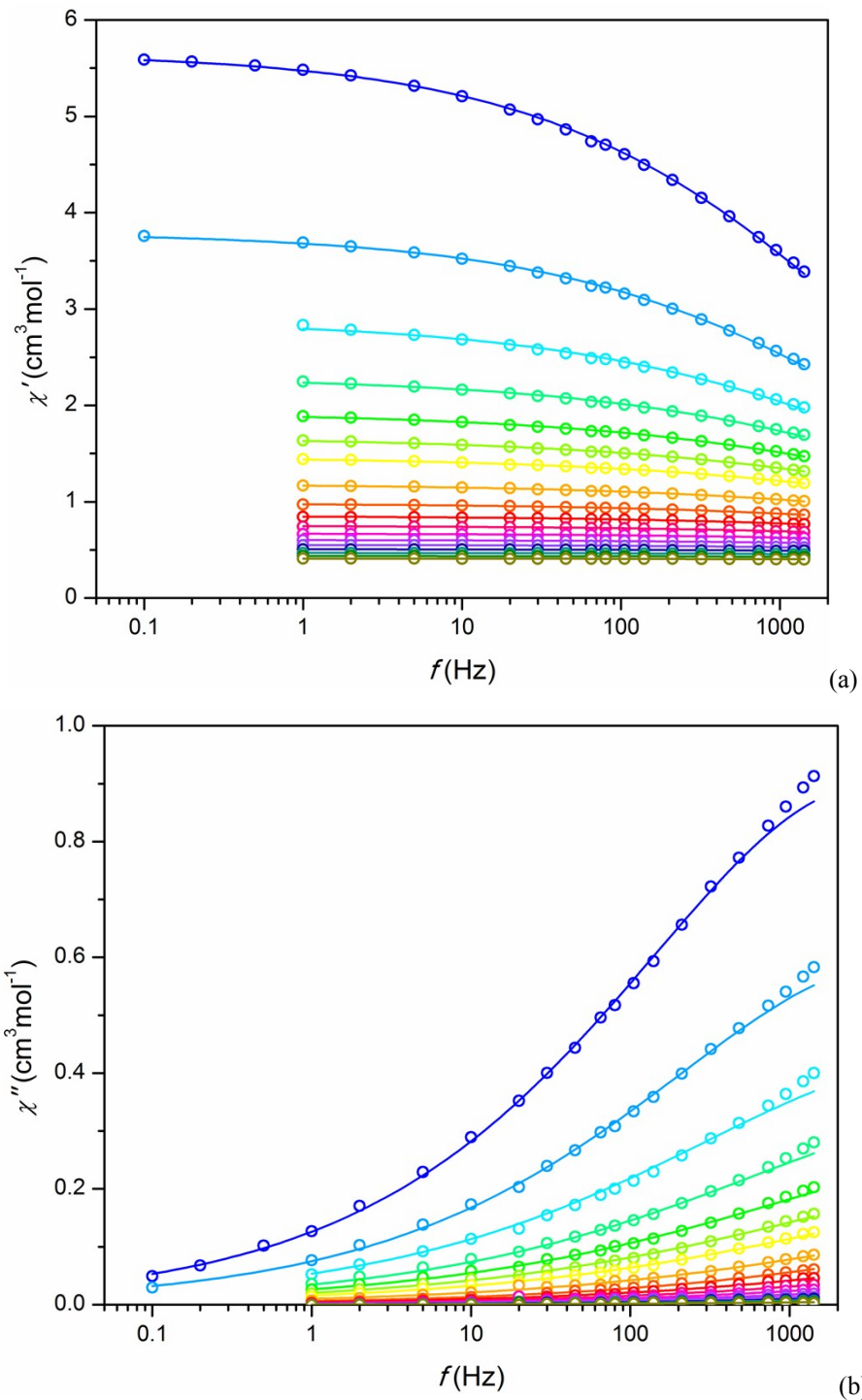
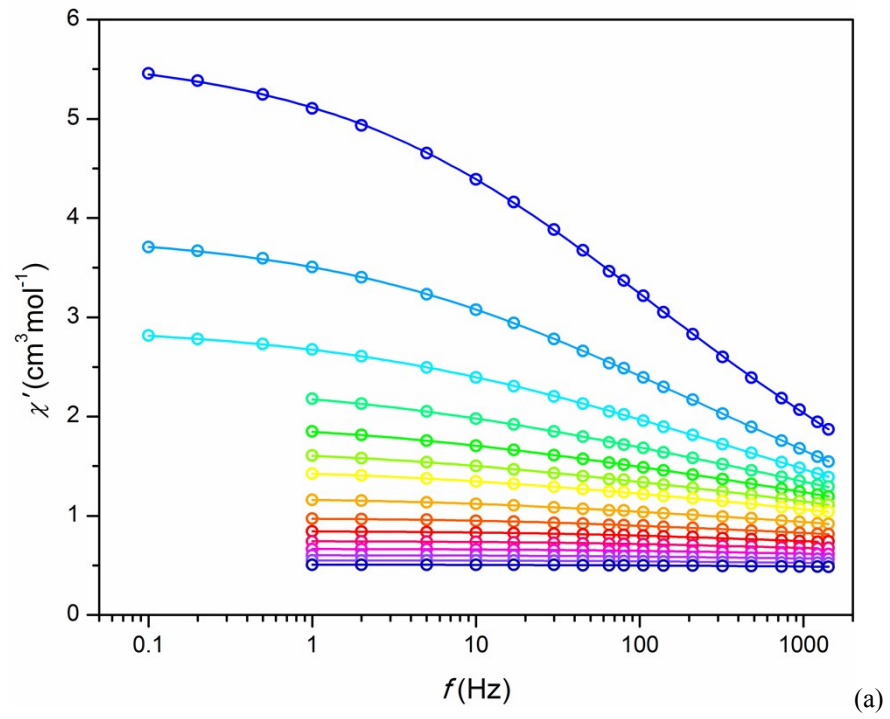
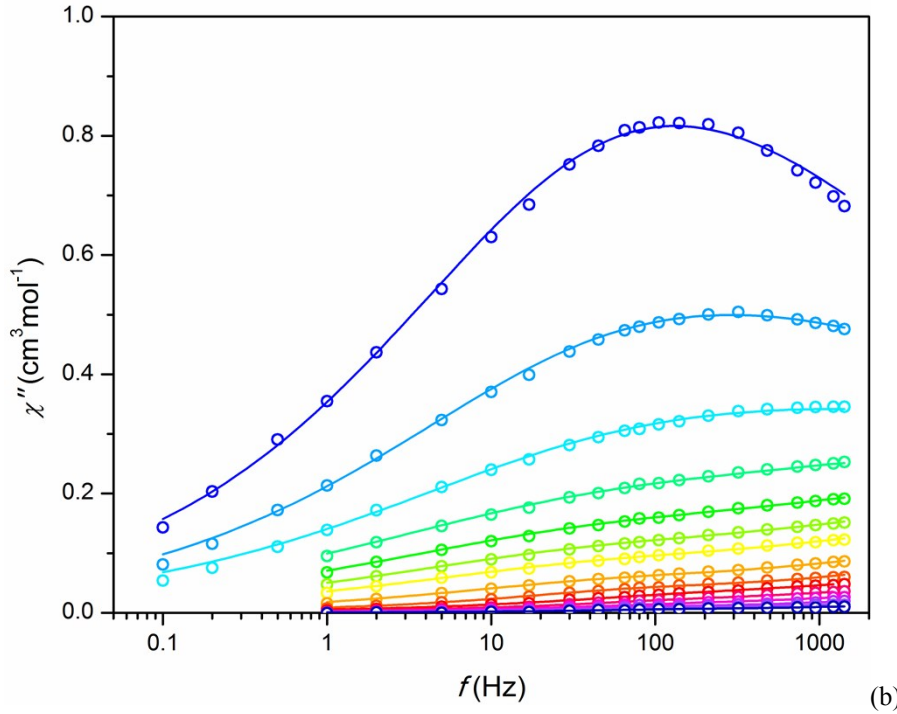


**Figure S3.** Frequency dependence of ac susceptibility per mol of Dy for **1** at different temperatures under a zero field. (a) – in-phase susceptibility  $\chi'$ , (b) – out-of-phase susceptibility  $\chi''$ . Symbols – experimental points, lines – fitting. Color designation: blue – green – red – navy – dark-yellow,  $T = 2 - 8 \text{ K}$  (step 1 K),  $T = 10 - 30 \text{ K}$  (step 2 K), respectively.

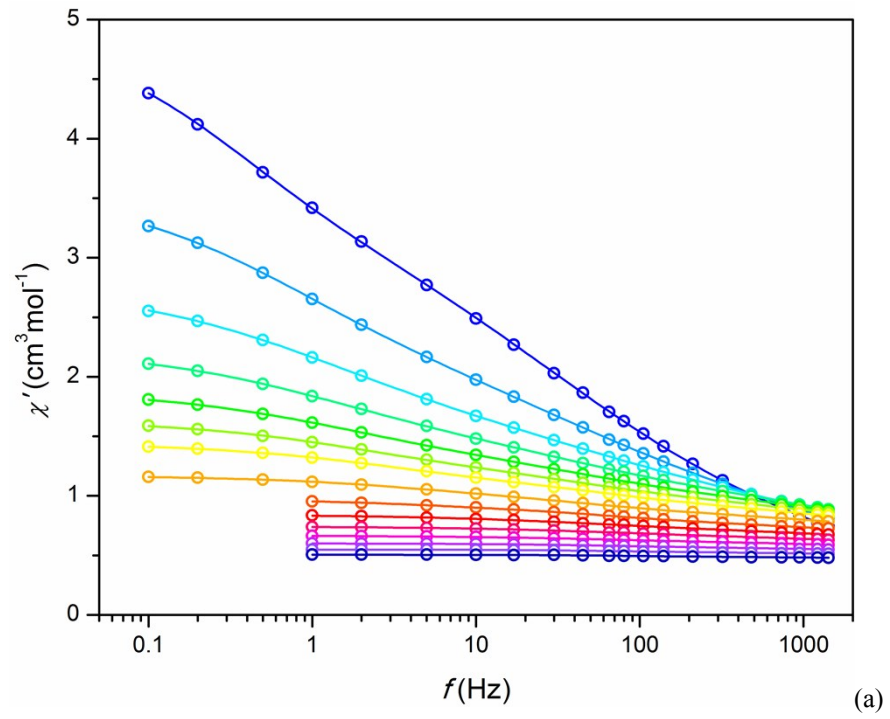


(a)

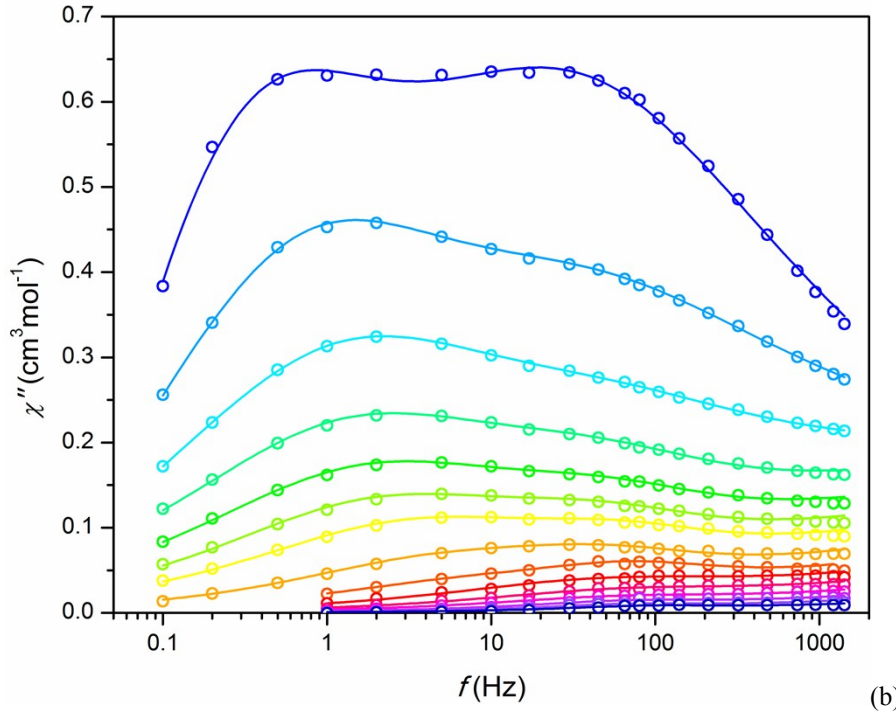


(b)

**Figure S4.** Frequency dependence of ac susceptibility per mol of Dy for **1** at different temperatures under a field of 0.4 kOe. (a) – in-phase susceptibility  $\chi'$ , (b) – out-of-phase susceptibility  $\chi''$ . Symbols – experimental points, lines – fitting. Color designation: blue – green – red – navy,  $T = 2 - 8 \text{ K}$  (step 1 K),  $T = 10 - 24 \text{ K}$  (step 2 K), respectively.



(a)



(b)

**Figure S5.** Frequency dependence of ac susceptibility per mol of Dy for **1** at different temperatures under a field of 1.5 kOe. (a) – in-phase susceptibility  $\chi'$ , (b) – out-of-phase susceptibility  $\chi''$ . Symbols – experimental points, lines – fitting. Color designation: blue – green – red – navy,  $T = 2 - 8 \text{ K}$  (step 1 K),  $T = 10 - 24 \text{ K}$  (step 2 K), respectively.

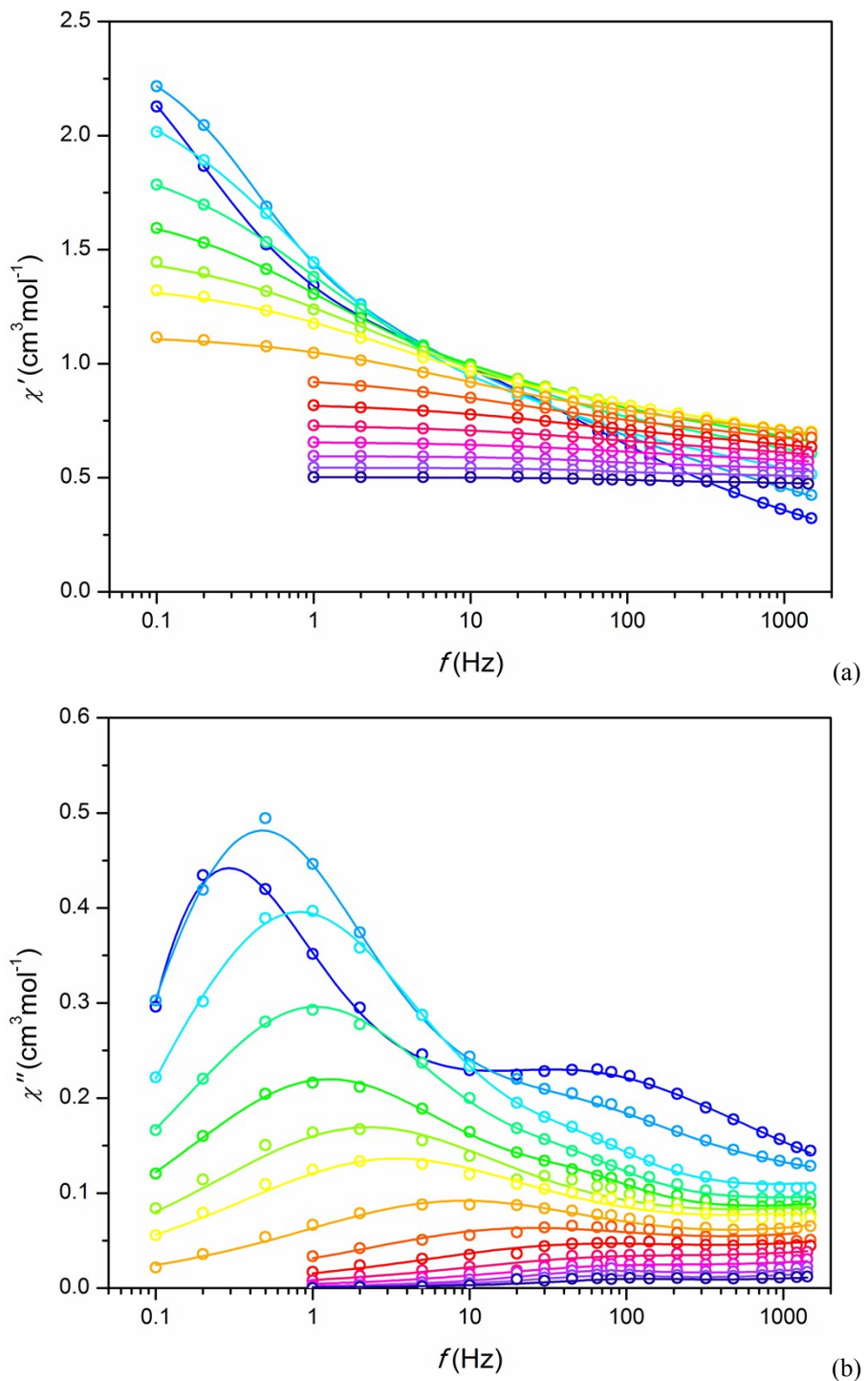
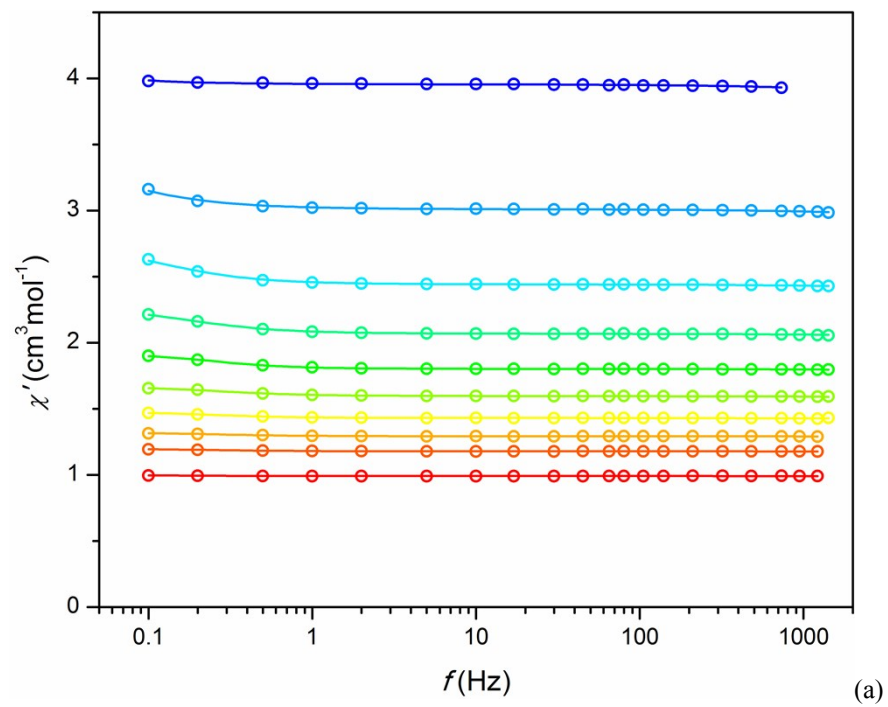
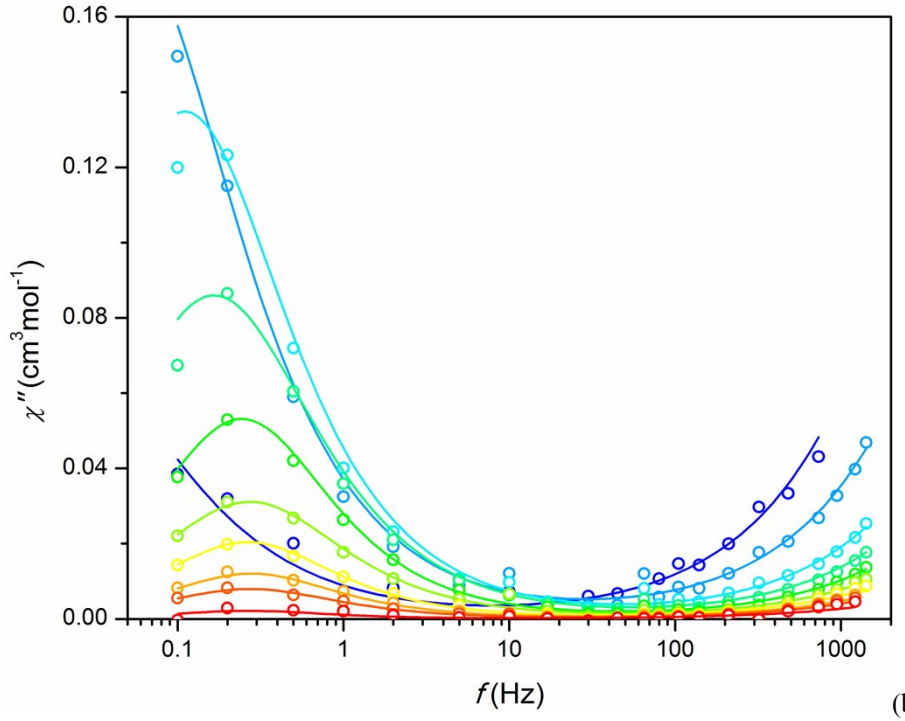


**Figure S6.** Frequency dependence of ac susceptibility per mol of Dy for **1** at different temperatures under a field of 4 kOe. (a) – in-phase susceptibility  $\chi'$ , (b) – out-of-phase susceptibility  $\chi''$ . Symbols – experimental points, lines – fitting. Color designation: blue – green – red – navy,  $T = 2 - 8 \text{ K}$  (step 1 K),  $T = 10 - 24 \text{ K}$  (step 2 K), respectively.



(a)



(b)

**Figure S7.** Frequency dependence of ac susceptibility per mol of Dy for **2** at different temperatures under a field of 1.5 kOe. (a) – in-phase susceptibility  $\chi'$ , (b) – out-of-phase susceptibility  $\chi''$ . Symbols – experimental points, lines – fitting. Color designation: blue – green – red,  $T = 2 - 10$  K (step 1 K), and  $T = 12$  K, respectively. Values of  $\chi_0$  (derived from dc magnetization measurements as differential susceptibilities) taken for the fitting: 4.310, 3.336, 2.658, 2.184 for  $T = 2, 3, 4, 5$  K, respectively.

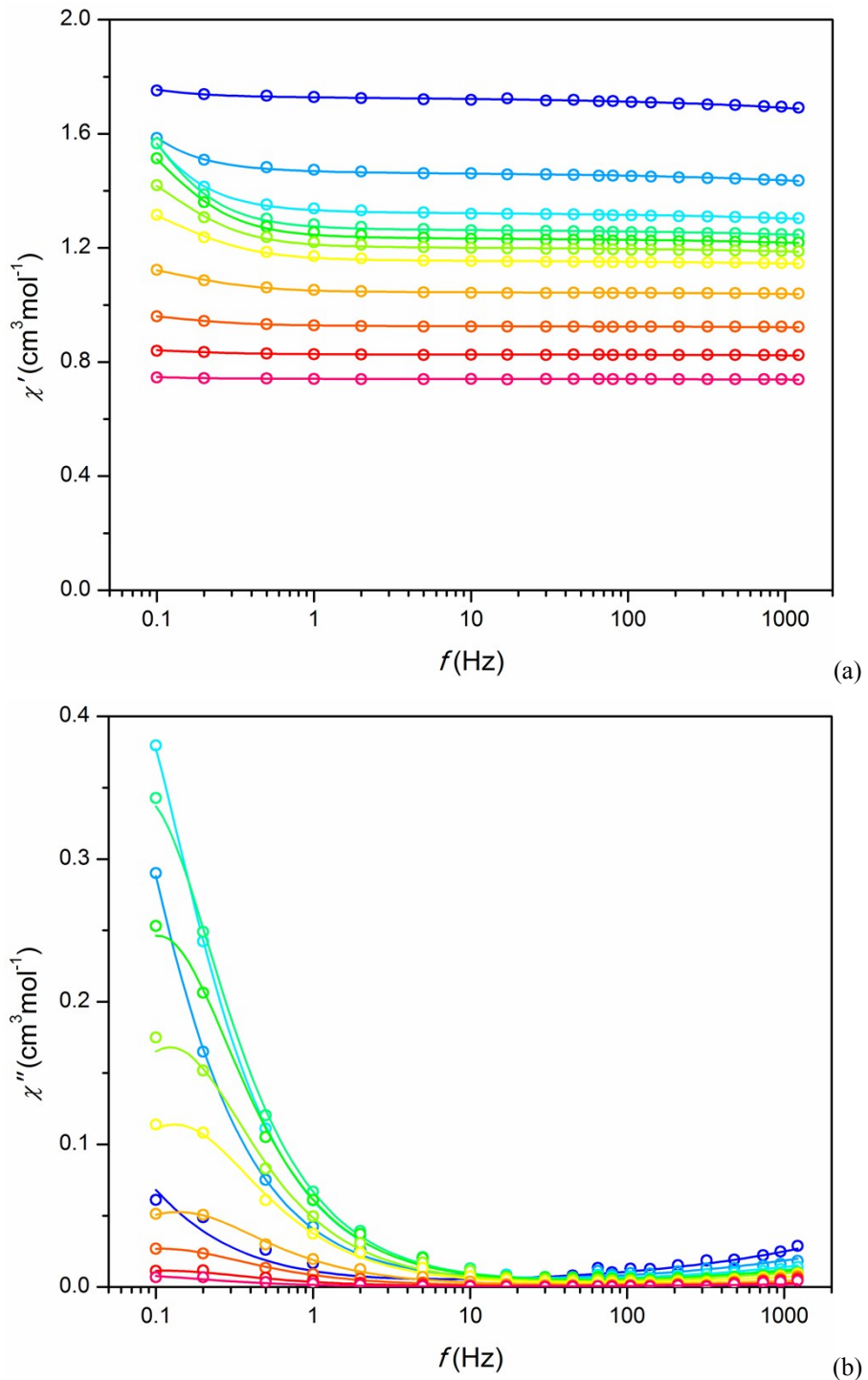


**Figure S8.** Frequency dependence of ac susceptibility per mol of Dy for **2** at different temperatures under a field of 4 kOe. (a) – in-phase susceptibility  $\chi'$ , (b) – out-of-phase susceptibility  $\chi''$ . Symbols – experimental points, lines – fitting. Color designation: blue – green – carmine-red,  $T = 2 - 8 \text{ K}$  (step 1 K),  $T = 10 - 16 \text{ K}$  (step 2 K), respectively. Values of  $\chi_0$  (derived from dc magnetization measurements as differential susceptibilities) taken for the fitting: 2.560, 2.465, 2.202, 1.922, 1.695, 1.500, 1.353, 1.117, for  $T = 2, 3, 4, 5, 6, 7, 8, 10 \text{ K}$ , respectively.

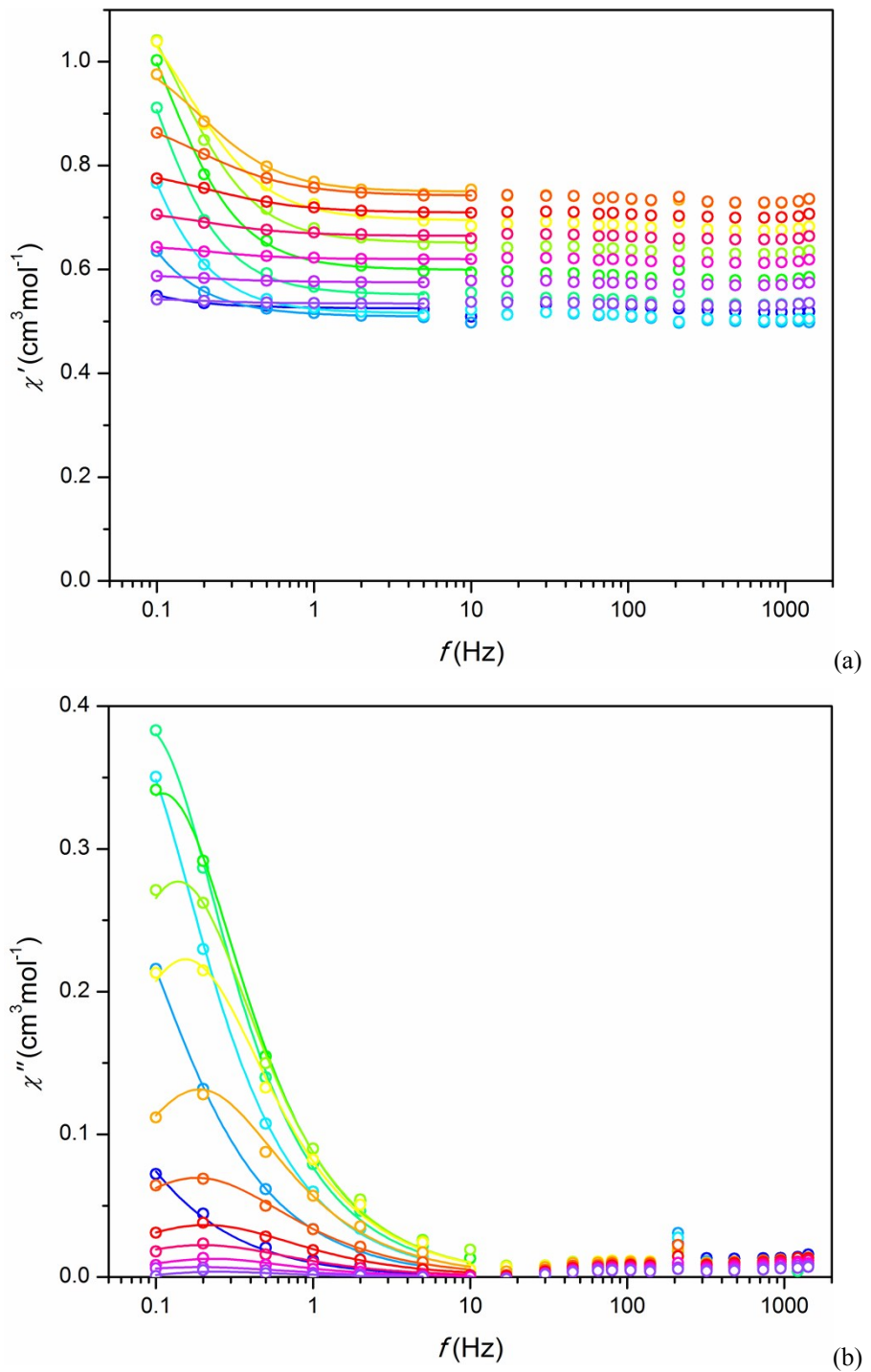


**Figure S9.** Frequency dependence of ac susceptibility per mol of Dy for **2** at different temperatures under a field of 8 kOe. (a) – in-phase susceptibility  $\chi'$ , (b) – out-of-phase susceptibility  $\chi''$ . Symbols – experimental points, lines – fitting. Color designation: blue – green – red – violet,  $T = 2 - 8 \text{ K}$  (step 1 K),  $T = 10 - 22 \text{ K}$  (step 2 K), respectively. Values of  $\chi_0$  (derived from dc magnetization measurements as differential susceptibilities) taken for the fitting: 0.906, 1.170, 1.303, 1.314, 1.277, 1.199, 1.140, 0.998, 0.875, 0.778, 0.696, for  $T = 2, 3, 4, 5, 6, 7, 8, 10, 12, 14, 16 \text{ K}$ , respectively.